

Chapter 14

Truncating the Impulse Responses of Substructures to Speed Up the Impulse-Based Substructuring

Daniel Rixen and Nazgol Haghighat

Abstract Recently a time-domain substructuring method was proposed based on the assembly of series of impulse responses of components: the Impulse Base Substructuring (IBS). Although theoretically the IBS is the time-domain equivalent to the Frequency Based Substructuring method (FBS), it has several advantages when computing shock responses for instance. However a major drawback of the IBS is the rapid increase of computational costs when the simulated time increases. In this contribution we propose a truncation and windowing procedure in order to limit the cost involved by the discretized convolution product inherent to the IBS method. We describe how to truncate the Impulse Response Functions of floating and non-floating substructures, and describe a cosine windowing function to improve the accuracy and stability of the dynamic response obtained from the superposition of truncated impulse responses. A simple bar example is used to illustrate the numerical performance of the truncated IBS.

14.1 Nomenclature

FRF	Frequency response functions
FBS	Frequency based substructuring
IBS	Impulse based substructuring
IRF	Impulse response functions
u	Array of degrees of freedom
f	Array of external forces
$H(t)$	Matrix of impulse response function
$\star^{(s)}$	Pertaining to substructure s
N^s	Number of substructures in the system
B	Signed Boolean matrix defining compatibility constraints
λ	Lagrange multipliers on interface
M, K, C	Mass, stiffness and damping matrix of a linear(ized) system
R	Matrix of rigid body modes of a floating substructure
dt	Time-step size
\star_n	Pertaining to time-step n
$[\star_i$	Component i of an array
β, γ	Parameters of the Newmark time-integration scheme
ε	Relative amplitude threshold for the truncation of the IRF
t_c	Cutoff time for the truncation of the IRF

D. Rixen (✉) • N. Haghighat
Faculty of Mechanics, Maritime and Material Engineering, Department of Precision and Microsystems Engineering,
Engineering Dynamics, Delft University of Technology, Mekelweg 2, 2628CD Delft, The Netherlands
e-mail: d.j.rixen@tudelft.nl

14.2 Introduction

The Impulse Based Substructuring (IBS) method was proposed in [3] as a time-domain counter-part of the Frequency Based Substructuring (FBS) (see for instance [1] for an overview of the FBS approach). The FBS represents the dynamics of the substructures through the Frequency Response Functions (FRFs) in the frequency domain at the interface, input and output degrees of freedom. The IBS describes the substructure dynamics using impulse response functions (IRF) which, in theory, are the inverse Fourier transforms of the FRFs.

Although the IBS approach is the direct counterpart of the FBS in the time domain, it has some advantages when one wants to compute the response of a system to shock loads using the measured or simulated response of its components.

In the present contribution we deal with one of the shortcomings of the IBS method, namely the fact that computing the response through a discretized convolution product can become computationally expensive when the time interval one is interested in for the simulation is not small. To alleviate the cost involved in the IBS computation, we investigate the possibility to apply truncation and windowing to the impulse responses of the components. Although such an approach seems straightforward, special caution must be taken when a component is floating, namely when it has not enough constraints to fix it in space once it is disconnected from its neighboring components.

In Sect. 14.2 we will shortly recall the basic principles of the IBS method and in Sect. 14.3 we discuss the truncation procedures for the IRFs of the components. We first describe the truncation and windowing for a non-floating component, then we develop a truncation procedure for floating ones. In Sect. 14.4 a simple numerical example is presented in order to illustrate the accuracy and stability of the solution computed by the truncated IBS approach.

14.3 The Impulse Based Substructuring in a Nutshell

14.3.1 Convolution of Impulse Response Functions and Inputs

The impulse based computation of the response of a dynamical system is described by the Duhamel's integral stating that a dynamic response is obtained from the convolution of the impulse response $h(t)$ (i.e. the response to a unit impulse at time $t = 0$) and the applied force $f(t)$. For a system with several inputs and outputs, we call $\mathbf{H}(t)$ the matrix of the impulse response functions between inputs and outputs. The system responses at the outputs are denoted by the array $\mathbf{u}(t)$ and the applied forces (the inputs) are denoted by an array $\mathbf{f}(t)$. The Duhamel's integral can then be written as

$$\mathbf{u}(t) = \int_0^t \mathbf{H}(t - \tau) \mathbf{f}(\tau) d\tau \quad (14.1)$$

In practice, for engineering systems, the IRFs, namely $\mathbf{H}(t)$ are not known analytically but can be measured (see [2]) or simulated (see [3]). So the IRF is available in a time-discretized form. Calling $\mathbf{H}_n, \mathbf{f}_n$ and \mathbf{u}_n , the IRF matrix, input and output arrays at time t_n , the Duhamel's integral (14.1) can be approximated by the finite difference form

$$\mathbf{u}_n = \sum_{i=0}^{n-1} (\mathbf{H}_{n-i} \mathbf{f}_i + \mathbf{H}_{n-i-1} \mathbf{f}_{i+1}) dt/2 \quad (14.2)$$

This approximation is obtained by applying the trapezoidal rule to the Duhamel's integral. It was observed in [3] that, if the IRF matrix is computed using a Newmark scheme, the discretization (14.2) yields the same dynamic response as when a Newmark scheme is applied to compute the response to the excitation \mathbf{f} .

14.3.2 Assembling the Dynamic Response of Substructures

Let us now assume that a system is described by the impulse response of its N_s substructures and let us call $\mathbf{H}^{(s)}$ the IRFs of substructure $\mathcal{Q}^{(s)}$. The assembly of the substructure is performed in a dual manner by imposing the compatibility between matching degrees of freedom on the interface between substructures. This can be written as

$$\sum_{s=1}^{N^s} \mathbf{B}^{(s)} \mathbf{u}^{(s)} = 0 \quad (14.3)$$

where $\mathbf{B}^{(s)}$ are signed Boolean matrices identifying the matching degrees of freedom on the interfaces (see [1] for instance). This relation merely states that for any matching pair $(u_i^{(s)}, u_j^{(r)})$ one must impose $u_i^{(s)} - u_j^{(r)} = 0$. This compatibility condition is enforced using Lagrange multipliers λ , representing the internal forces on the interfaces. Hence for a partitioned problem the Duhamel's integral (14.1) can be written as¹

$$\left\{ \begin{array}{l} \mathbf{u}^{(s)}(t) = \int_0^t \mathbf{H}^{(s)}(t-\tau) \left(\mathbf{f}^{(s)}(\tau) + \mathbf{B}^{(s)T} \lambda(\tau) \right) d\tau \\ \sum_{s=1}^{N^s} \mathbf{B}^{(s)} \mathbf{u}^{(s)}(t) = 0 \end{array} \right. \quad (14.4)$$

Considering the same time-discretization as in (14.2), taking into account that $\mathbf{H}_0 = \mathbf{0}$, the dual assembly (14.4) can be discretized as

$$\left\{ \begin{array}{l} \mathbf{u}^{(s)}_n = \mathbf{H}_n^{(s)} \left(\mathbf{f}_0^{(s)} \frac{dt}{2} + \mathbf{B}^{(s)T} \lambda_0 \right) + \sum_{i=1}^{n-1} \mathbf{H}_{n-i}^{(s)} \left(\mathbf{f}_i^{(s)} dt + \mathbf{B}^{(s)T} \lambda_i \right) \\ \sum_{s=1}^{N^s} \mathbf{B}^{(s)} \mathbf{u}_n^{(s)} = 0 \end{array} \right. \quad (14.5)$$

In practice this system is solved for every time instance t_n by first predicting the substructure response as if the interface impulses λ_{n-1} are null, then computing the λ_{n-1} necessary to satisfy compatibility at time t_n , and finally correcting the substructure responses for the interface force. In summary,

$$\tilde{\mathbf{u}}_n^{(s)} = \mathbf{H}_n^{(s)} \left(\mathbf{f}_0^{(s)} \frac{dt}{2} + \mathbf{B}^{(s)T} \lambda_0 \right) + \sum_{i=1}^{n-2} \mathbf{H}_{n-i}^{(s)} \left(\mathbf{f}_i^{(s)} dt + \mathbf{B}^{(s)T} \lambda_i \right) + \mathbf{H}_1^{(s)} \mathbf{f}_{n-1}^{(s)} dt \quad (14.6)$$

$$\lambda_{n-1} = - \left(\sum_{s=1}^{N^s} \mathbf{B}^{(s)} \mathbf{H}_1^{(s)} \mathbf{B}^{(s)T} \right)^{-1} \sum_{s=1}^{N^s} \mathbf{B}^{(s)} \tilde{\mathbf{u}}_n^{(s)} \quad (14.7)$$

$$\mathbf{u}_n^{(s)} = \tilde{\mathbf{u}}_n^{(s)} + \mathbf{H}_1^{(s)} \mathbf{B}^{(s)T} \lambda_{n-1} \quad (14.8)$$

14.4 Truncating the Impulse Responses

Clearly the cost of the discretized convolution (14.6) is increasing rapidly when the simulation time t_n is getting large. This is due to the fact that all the forces that have been acting on the system from time t_0 to time t_{n-1} determine the dynamic response at t_n through the history transmitted over the time domain according to the impulse response \mathbf{H} . For instance the force \mathbf{f}_0 applied at time t_0 will influence the response at time t_n through the value of the IRFs \mathbf{H}_n . If however the IRFs at t_n have significantly decreased due to the damping in the system, it seems acceptable to neglect the contribution of \mathbf{f}_0 to the response \mathbf{u}_n . In essence one then truncates the IRFs of the system. This will be investigated in this section, first for a non-floating component, then for a floating component.

¹ In the time-discrete form λ are chosen to represent interface impulses.

14.4.1 Non-Floating Substructures

Let us split the Duhamel's integral (14.2) in the following two convolution products:

$$u_n = \int_0^{t_n} H(t_n - \tau)f(\tau) d\tau = \int_0^{t_n - t_c} H(t_n - \tau)f(\tau) d\tau + \int_{t_n - t_c}^{t_n} H(t_n - \tau)f(\tau) d\tau \quad (14.9)$$

Let us further assume that after time t_c the IRFs have decayed so that they can be assumed to be zero:

$$H(t_n - \tau) \simeq 0 \quad \text{for } t_n - \tau > t_c, \text{ namely for } \tau < t_n - t_c$$

Note that this will occur only if damping is present and if the structure is not floating. Indeed if the structure (or substructure in the case of the IBS) are not restrained by enough imposed displacements, the IRFs will grow steadily due to the rigid body motion generated by the initial impulse. This case will be discussed in Sect. 14.3.2. Assuming thus that enough damping is present and that the (sub)structure is not floating, one can then write the approximation²

$$u_n \simeq \int_{\max\{0, t_n - t_c\}}^{t_n} H(t_n - \tau)f(\tau)d\tau \quad (14.10)$$

$$\simeq \sum_{i=\max\{0, n-c\}}^{n-1} (H_{n-i}f_i + H_{n-i-1}f_{i+1})dt/2 \quad (14.11)$$

This approximation can significantly reduce the cost of the convolution computation. It corresponds to cutting the IRF after time t_c , and can thus be seen as windowing the IRF with a rectangular window of width equal to t_c . Obviously other windows can be defined in order to force the IRFs to zero in a smoother manner. This is discussed next.

Let us consider a user defined threshold ε . Then the cutoff time t_c can be chosen as the time for which all the impulse responses in \mathbf{H} have a vibrational amplitude lower than ε (see Fig. 14.1). The approximation (14.11) can then be interpreted as applying a rectangular window on the IRFs in order to set them to zero after time t_c . Such a rectangular window can formally be written as

$$W_{rect}(t) = \begin{cases} 1 & \text{if } t < t_c \\ 0 & \text{if } t > t_c \end{cases} \quad (14.12)$$

where t_c is such that the amplitude of all the IRFs in \mathbf{H} have reached an oscillatory amplitude ε -times lower than their maximum value over time.³ Obviously, forcing the impulse response to zero can seriously perturb the dynamic response computed by superposition of impulse responses since it corresponds to introducing parasitic impulses after time t_c in order to “kill” the impulse response of forces that have been acting on the system c time steps earlier. Thus applying smoother windows is desirable in order to improve the accuracy and the stability of the dynamic response constructed on truncated IRFs. Here we will investigate a simple *cosine* window defined as

$$W_{cos}(t) = \begin{cases} \cos\left(\frac{\pi t}{2t_c}\right) & \text{if } t < t_c \\ 0 & \text{if } t > t_c. \end{cases} \quad (14.13)$$

An illustration of such a window is given in Fig. 14.2. This cosine window has the advantage to introduce only very small additional damping at the beginning of the IRF, therefore not perturbing to much the dynamical properties of the system.

² In case of substructures, one must also add the interface forces $B^{(s)\top} \lambda$ in these equations. Nevertheless, to simplify the text, we will omit the interface forces in this section.

³ In our work the oscillatory amplitude is detected by evaluating the peak values of the IRFs.

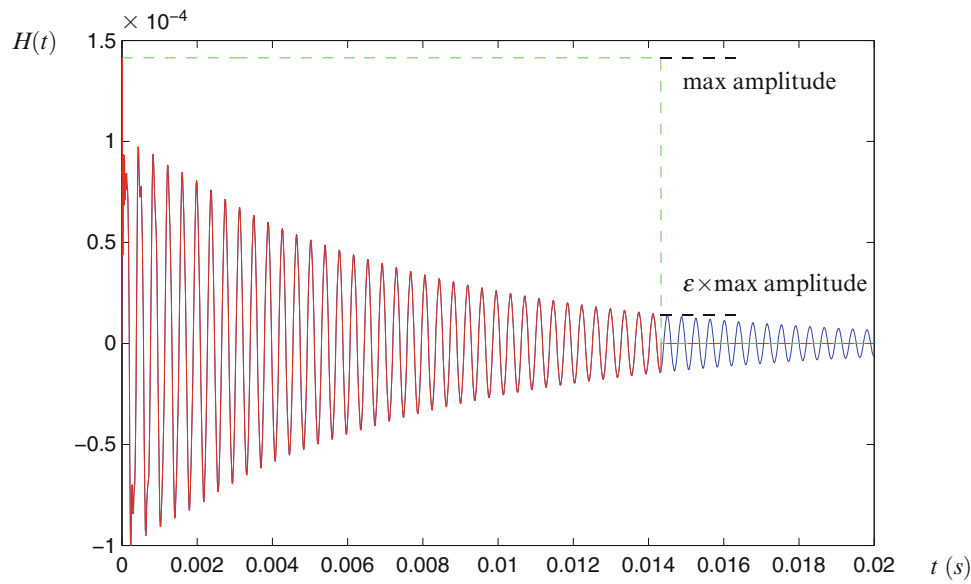


Fig. 14.1 IRF truncated by a rectangular window

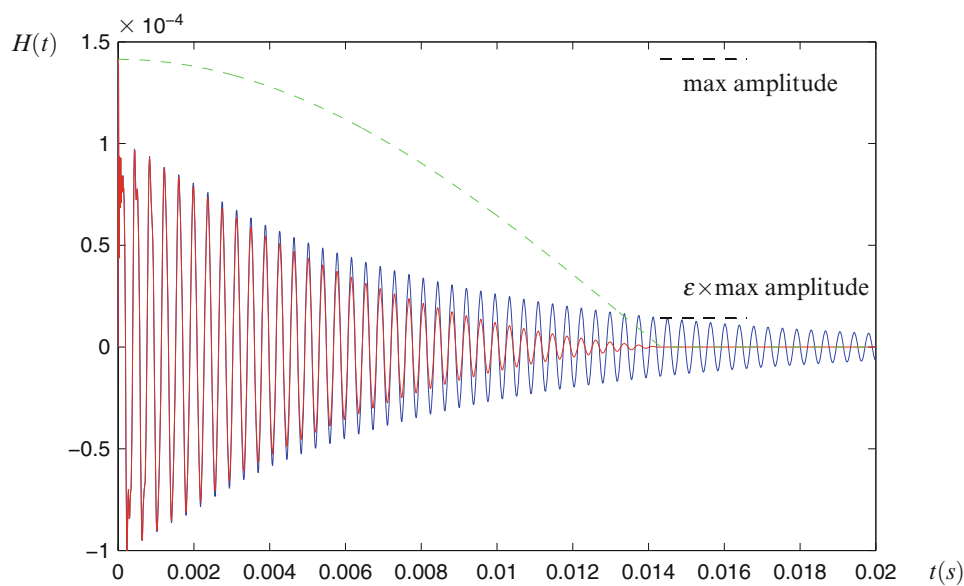


Fig. 14.2 IRF truncated by a cosine window

Nevertheless one should be aware that such a window, unlike for instance a classical exponential window, transforms the IRF in a dynamic response that is not mechanically interpretable. Furthermore, the high slope of the cosine window close to the cutoff time might induce significant velocity and acceleration perturbations.

When such a non-rectangular window is applied one first multiplies the IRFs up to t_c by W_{cos} to obtain the weighted IRFs \bar{H} (red curve in Fig. 14.2) and uses the truncated convolution (14.11) where H is replaced by \bar{H} . Obviously such a procedure can be introduced in the IBS approach (14.5) by simply restricting the convolution computation and replacing the IRFs by the weighted ones.

14.4.2 Floating Substructures

Let us now consider the case of a floating (sub)structure and split again the convolution product as in (14.9)

$$u_n = \int_0^{t_n} H(t_n - \tau)f(\tau) d\tau = \int_0^{t_n - t_c} H(t_n - \tau)f(\tau) d\tau + \int_{t_n - t_c}^{t_n} H(t_n - \tau)f(\tau) d\tau$$

When the substructure is floating, namely when there are not enough boundary conditions to block its rigid body motion, one can no longer assume that the IRF is close to zero after a time t_c since the initial impulse has generated an initial velocity causing the (sub)structure to drift away. In fact the IRF can be seen as a vibration superimposed on a global rigid body motion.

The approach proposed here is then to truncate and apply a window on the part of the IRF remaining when one has removed the rigid body motion due to a unit impulse. The overall rigid body motion in the IRF will be accounted for during the full length of the convolution and thus is not truncated.

To build the rigid body response, one can either estimate the constant velocity part from the measured or simulated IRF, or if the global inertia of the (sub)structure is known, it can be computed. Calling \mathbf{R} the matrix containing in its columns the rigid body modes of the (sub)structure (i.e. the nullspace of the stiffness matrix \mathbf{K}), the overall motion is found by setting

$$u = R\alpha \quad (14.14)$$

where α are the unknown rigid body mode amplitudes. Let us write the linear(ized) equilibrium equation of the system as

$$M\ddot{u} + C\dot{u} + Ku = f \quad (14.15)$$

where \mathbf{M} , \mathbf{C} and \mathbf{K} are respectively the mass, damping and stiffness matrices. Introducing the assumption (14.14) in the equilibrium equation and noting that $\mathbf{KR} = \mathbf{0}$ by definition, and assuming further that $\mathbf{CR} = \mathbf{0}$,⁴ one finds

$$R^T MR\ddot{\alpha} = R^T f \quad (14.16)$$

Thus, when f is an initial unit impulse, one can write

$$\int_0^t \int_0^t R^T MR\ddot{\alpha} dt = \int_0^t \int_0^t R^T f = R^T \mathbf{1} \mathbf{1} t$$

where $\mathbf{1}$ is an array containing zeros for all entries except at the degree of freedom excited by the impulse, where the value of $\mathbf{1}$ is 1. Defining then

$$M_{tot} = R^T MR \quad (14.17)$$

the total inertia related to the rigid body modes \mathbf{R} and recalling that for the IRF, initial conditions are null, one finds

$$\alpha = M_{tot}^{-1} R^T \mathbf{1} \mathbf{1} t \quad (14.18)$$

Substituting now in (14.14) one finds the rigid body motion related to a unit impulse:

$$u_{rigid} = R_{tot}^{-1} R^T \mathbf{1} \mathbf{1} t \quad (14.19)$$

So computing the rigid body motion associated to every input of the IRF matrix \mathbf{H} , one builds the rigid body response matrix

⁴This assumption means that the damping in the (sub)structure is internal and does not produce any damping force when no deformations are present.

$$H^{rig} = RM_{tot}^{-1}R^T t \quad (14.20)$$

and the vibrational part of the IRF is obtained from⁵

$$H^{vib} = H - H^{rig} \quad (14.21)$$

The truncation of the IRF for a floating (sub)structure then consists in truncating only its vibrational part since that portion of the IRF can be assumed to decay to a negligible contribution after the cutoff time t_c . Mathematically speaking we write

$$\begin{aligned} n &= \int_0^{t_n} H(t_n - \tau)f(\tau) d\tau \\ &= \int_0^{t_n} (H^{rig}(t_n - \tau) + H^{vib}(t_n - \tau))f(\tau) d\tau \\ &\simeq \int_0^{t_n} {}^{rig}(t_n - \tau)f(\tau)d\tau + \int_{t_n-t_c}^{t_n} {}^{vib}(t_n - \tau)f(\tau) d\tau \\ &\text{where } {}^{rig}(t_n - \tau) = R_{tot}^{-1}R^T [t_n - \tau] d\tau \end{aligned} \quad (14.22)$$

The first part represents the rigid body response to the force f and, introducing the simplified notation

$$\mathcal{M}^{-1} = RM_{tot}^{-1}R^T, \quad (14.23)$$

it can be written as

$$\begin{aligned} u_n^{rig} &= \int_0^{t_n} \mathcal{M}^{-1} [t_n - \tau]f(\tau) d\tau \\ &= \int_0^{t_{n-1}} \mathcal{M}^{-1} [t_{n-1} + dt - \tau]f(\tau) d\tau + \int_{t_{n-1}}^{t_n} \mathcal{M}^{-1} [t_n - \tau]f(\tau)d\tau \\ &= \int_0^{t_{n-1}} \mathcal{M}^{-1} [t_{n-1} - \tau]f(\tau)\tau + \mathcal{M}^{-1} dt \int_0^{t_{n-1}} f(\tau) d\tau + \mathcal{M}^{-1} \int_{t_{n-1}}^{t_n} [t_n - \tau]f(\tau)d\tau \\ &= u_{n-1}^{rig} + \mathcal{M}^{-1} \left\{ dt \int_0^{t_{n-1}} f(\tau) d\tau + \int_{t_{n-1}}^{t_n} [t_n - \tau]f(\tau)d\tau \right\} \end{aligned} \quad (14.25)$$

This last relation is interesting since it indicates that the rigid body part of the response can be computed by time stepping and does not need a lengthy convolution. Let us observe that the second term in (14.25) can be given a clear physical interpretation by noting that $\mathcal{M}^{-1} \int_0^{t_{n-1}} f(\tau) d\tau$, basically the accumulated impulses divided by the inertia, corresponds to the overall velocity at time t_{n-1} . So the second term expresses the increase of displacement during the time increment dt due to that velocity. The third term is related to the additional acceleration produced by the force applied between t_{n-1} and t_n .

The discretization of (14.25) can be performed using the same finite difference approach as done earlier for the convolution product. For that let us restart from the definition (14.24) of the rigid response and discretize it in time following the trapezoidal rule also used in (14.2):

⁵ Let us note that since the impulse response for a linear dynamic system can be seen as the superposition of its impulse modal responses, an equivalent way to compute the vibrational part of the IRF is to project the IRF M -orthogonal to the rigid body modes, namely

$$H^{vib} = (I - RM_{tot}^{-1}R^T)H$$

and the rigid part is

$$H^{rig} = R M_{tot}^{-1}R^T H$$

$$\begin{aligned}
u_n^{rig} &= \int_0^{t_n} \mathcal{M}^{-1} [t_n - \tau] f(\tau) \tau \\
&\simeq \mathcal{M}^{-1} \sum_{i=0}^{n-1} \left\{ [(n \, dt - \tau) f(\tau)]_{\tau=i \, dt} + [(n \, dt - \tau) f(\tau)]_{\tau=(i+1) \, dt} \right\} \frac{dt}{2} \\
&\simeq \mathcal{M}^{-1} \sum_{i=0}^{n-1} \left\{ (n-i) f_i + (n-i-1) f_{i+1} \right\} \frac{dt^2}{2}
\end{aligned} \tag{14.26}$$

Following now the same steps as from (14.24) to (14.25), but now in the time-discrete case,

$$\begin{aligned}
u_n^{rig} &\simeq \mathcal{M}^{-1} \sum_{i=0}^{n-1} \left\{ (n-i) f_i + (n-i-1) f_{i+1} \right\} \frac{dt^2}{2} \\
&\simeq \mathcal{M}^{-1} \sum_{i=0}^{n-2} \left\{ (n-i) f_i + (n-i-1) f_{i+1} \right\} \frac{dt^2}{2} + \mathcal{M}^{-1} f_{n-1} \frac{dt^2}{2} \\
&\simeq \mathcal{M}^{-1} \sum_{i=0}^{n-2} \left\{ ((n-1)-i) f_i + ((n-1)-i-1) f_{i+1} \right\} \frac{dt^2}{2} + \mathcal{M}^{-1} \sum_{i=0}^{n-2} \{ f_i + f_{i+1} \} \frac{dt^2}{2} + \mathcal{M}^{-1} f_{n-1} \frac{dt^2}{2} \\
&\simeq u_{n-1}^{rig} + \mathcal{M}^{-1} \sum_{i=0}^{n-2} \{ f_i + f_{i+1} \} \frac{dt^2}{2} + \mathcal{M}^{-1} f_{n-1} \frac{dt^2}{2}
\end{aligned} \tag{14.27}$$

which reveals the time-discrete form of (14.25). Finally we can summarize the discretized and truncated IRFs for floating domains by substituting in (14.22) the discretization (14.27) for the rigid part and considering the truncation (14.11) for the vibrational term:

$$\mathcal{I}_0 = f_0 \frac{dt}{2} \tag{14.28}$$

$$\mathcal{I}_n = \mathcal{I}_{n-1} + f_{n-1} \, dt \tag{14.29}$$

$$u_n^{rig} = u_{n-1}^{rig} + \mathcal{M}^{-1} \mathcal{I}_n \, dt \tag{14.30}$$

$$u_n \simeq u_n^{rig} + \sum_{i=\max\{0, n-c\}}^{n-1} (\bar{H}_{n-i}^{vib} f_i + \bar{H}_{n-i-1}^{vib} f_{i+1}) dt/2 \tag{14.31}$$

where the effect of the applied forces is accumulated in the total impulse \mathcal{I}_n and where \bar{H}^{vib} denotes the vibrational part of the IRFs possibly weighted by, for instance, the cosine window described in the previous section. In the context of the IBS, the truncation of the convolution product for floating subdomains can be introduced in the dually assembled form (14.5).

14.5 A Simple Example

In this contribution we consider the same example as the one treated in [3]. We consider the bar structure described in Fig. 14.3 excited by a load at its end. The structure is divided in two substructures of equal length, each substructure being modeled by 25 bar finite elements (the consistent mass matrices are used here). The bar is made of steel ($E = 2.1 \cdot 10^{11}$ Pa, $\rho = 7500$ kg/m³), has a uniform cross-section of $A = 3.14 \cdot 10^{-4}$ m² and each substructure has a length of $L = 0.5$ m. In the model damping has been introduced by constructing $C = 1 \cdot 10^{-6}$ K.

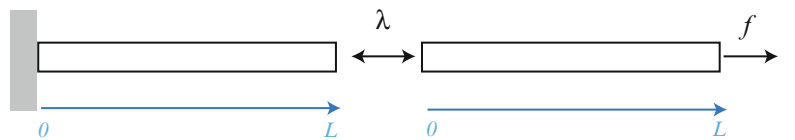


Fig. 14.3 Example of a beam with two substructures

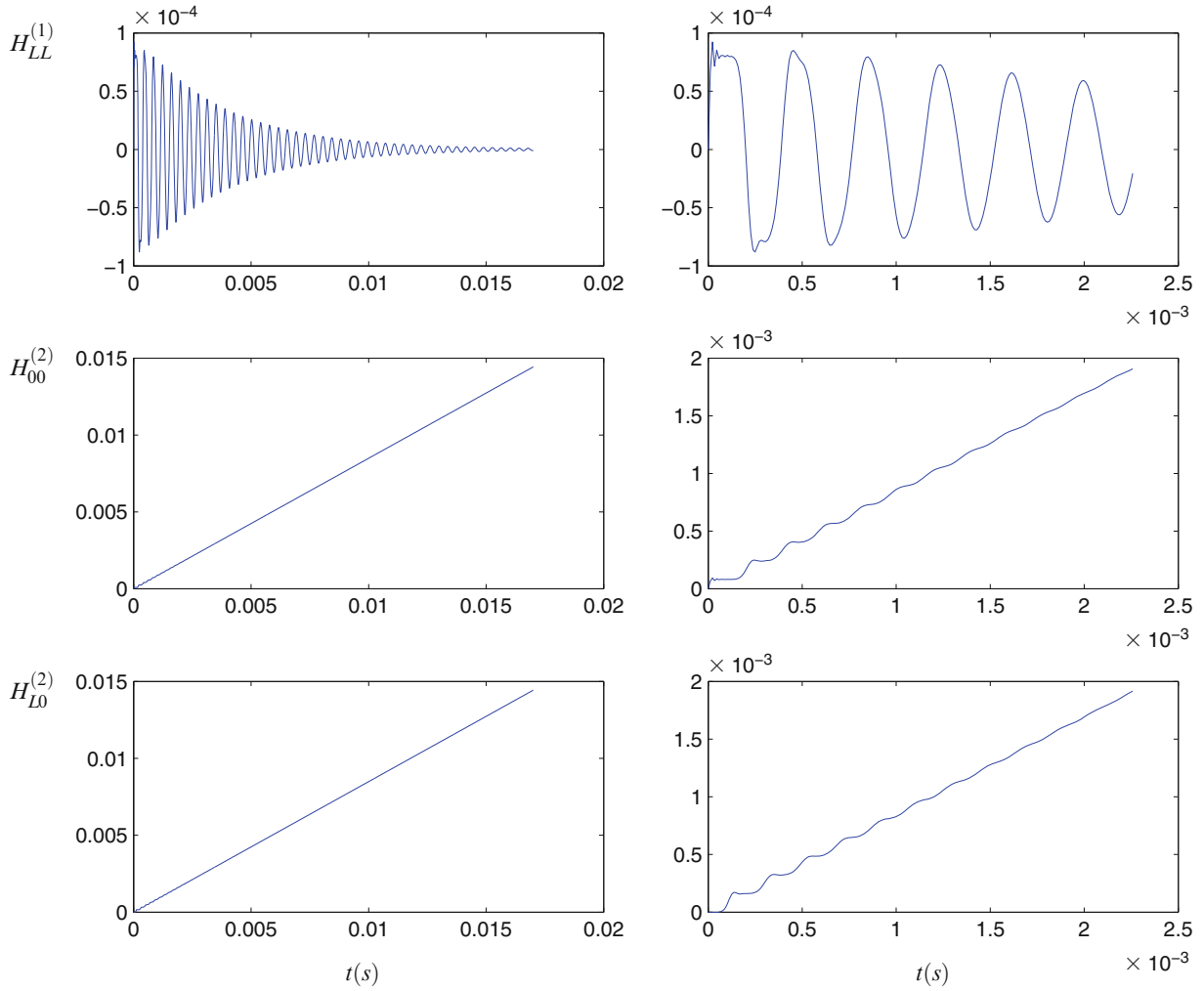


Fig. 14.4 IRFs for the bar substructures (zoomed on the *right*)

Assuming the dofs of the substructures are numbered from left to right, the Boolean constraining matrices are

$$B^{(1)} = [0 \cdots 0 \ 1]$$

$$B^{(2)} = [1 \cdots 0 \ 0]$$

The impulse responses are computed using a Newmark scheme $\gamma = 1/2, \beta = 1/4$ for a unit force applied at time $t = 0$ at the interface degrees of freedom and at the end of the second substructure (this will be the input of the force in our example). The time-step is chosen equal to $3dt_{crit}$ where dt_{crit} is the critical time step, namely the stability limit if the integration scheme would be explicit. The obtained IRFs are plotted in Fig. 14.4 for inputs on the interface and on the end of the bar. On the right of that figure the IRFs are zoomed. The IRFs for this problem are shown in Fig. 14.4. It can be clearly seen that the IRFs for the right substructure converge to a monotonically increasing line, illustrating the drift of the displacement for a floating substructure. In this case the rigid body mode of the second substructures is simply an array with all ones as entries and the total mass matrix M_{total} is equal to the total translation mass of the second substructure.

Now, using the IBS approach described by (14.7), we compute the response of the assembled bar to a step load of unit amplitude applied at the right end (see [3] for a detailed outline of the algorithm for this example). The threshold ε for the truncation (see Sect. 14.3.1, Figs. 14.1 and 14.2) was chosen successively to be 10^{-1} , 10^{-2} and 10^{-3} .

In Fig. 14.5 we report the dynamic response obtained at the interface of the bar, under a unit step load applied at the end of the bar, when applying the IBS approach with and without truncation. Here a simple rectangular window is applied (as illustrated in Fig. 14.1). When the threshold ε is chosen to high (in this case $\varepsilon = 10^{-1}$) the truncation introduces too many

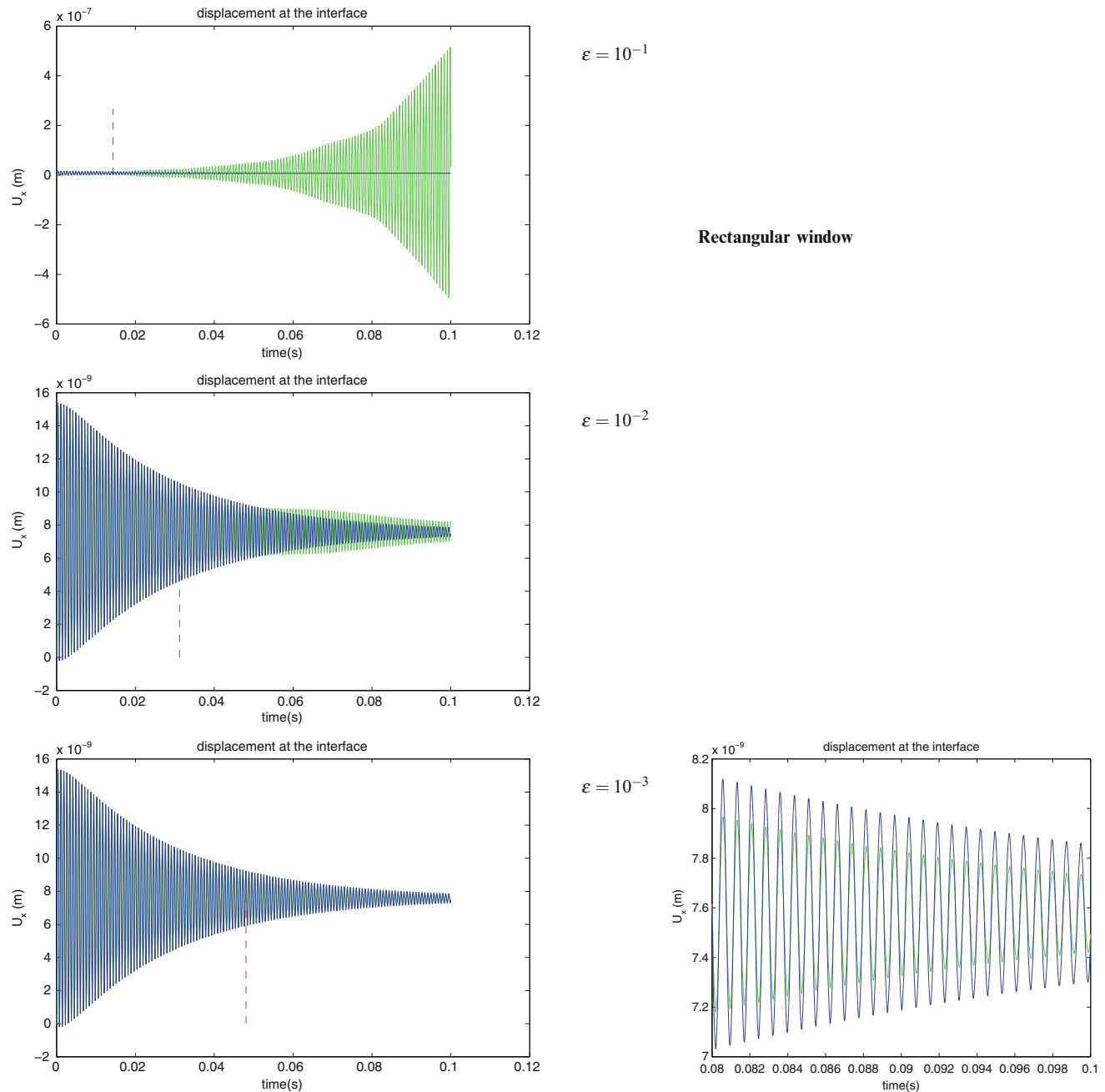


Fig. 14.5 Interface displacement of the full bar to a unit step, computed by IBS, with (green) and without (blue) truncation: rectangular window. The red line indicates the cutoff time for the truncation

residual impulses leading to an unstable response in the IBS. For $\varepsilon = 10^{-2}$ the solution is stable, but clearly the truncation significantly affects the accuracy of the solution. For $\varepsilon = 10^{-3}$, the solution computed by the truncated IBS is rather accurate, although zooming in the curves (right side of Fig. 14.5) it is clear that a noticeable error has been introduced by the truncation. Note that for this last case, namely $\varepsilon = 10^{-3}$, the cutoff time is $t_c = 0.048$, resulting in only a small computational saving in our computation where the simulation is run until $t_{final} = 0.1$.

Applying now a cosine window, we obtain the results reported in Fig. 14.6. It is very interesting to observe that with the cosine window the IBS method results in a stable and rather accurate dynamic response, even for $\varepsilon = 10^{-1}$. This threshold corresponds to a cutoff time $t_c = 0.014$ and the truncation yields a significant reduction of computational effort in computing the convolution product. Finally we observe that when the threshold is further reduced (to 10^{-2} and 10^{-3}) the results of the truncated IBS is nearly identical to the results without truncation. Nevertheless the cutoff time is higher and thus more computational effort is required.

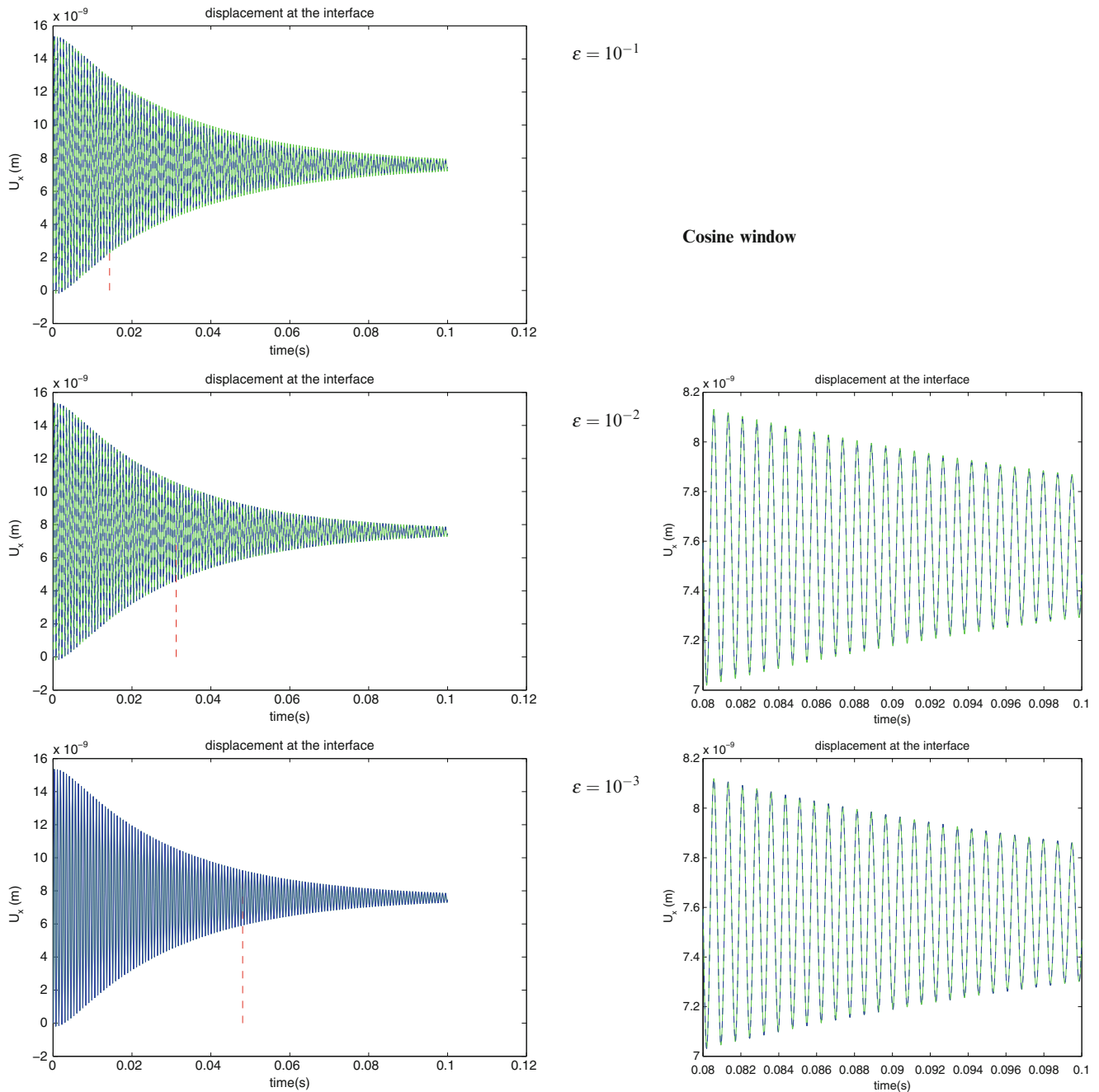


Fig. 14.6 Interface displacement of the full bar to a unit step, computed by IBS, with (green) and without (blue) truncation: cosine window. The red line indicates the cutoff time for the truncation (color figure online)

14.6 Conclusion

In this contribution we have shown how to apply truncation and windowing on the Impulse Response Functions (IRF) of substructures, so that one can significantly reduce the computational burden related to the convolution product in the Impulse Based Substructuring (IBS) method.

Special care must be taken when truncating the IRFs of floating substructure: the overall rigid body motion can not be truncated since it does not decay to zero. We have indicated how the truncation can be applied only to the vibrational part of the IRF in that case.

We have described a cosine window in order to force the IRF smoothly to zero at the cutoff time, without introducing significant damping in the system. The results on a simple bar example decomposed in two substructures have indicated that the truncated IBS with the cosine window can produce accurate results while significantly reducing the necessary number of operations in the computation of the convolution product.

Future work will concentrate on investigating other time windows and on applying windowing directly on the IRF expressed for the velocities or the accelerations. Also more detailed analysis must be performed to investigate the stability conditions for the truncated IBS. Currently, the truncated IBS is being applied to a three-dimensional engineering structure in order to estimate the gain in computational time when applying an appropriate truncation.

References

1. Klerk DD, Rixen DJ, Voormeeren SN (2008) General framework for dynamic substructuring: history, review and classification of techniques. *AIAA J* 46(5):1169–1181
2. Rixen DJ (2010) Substructuring technique based on measured and computed impulse response functions of components. In: Sas P, Bergen B (eds) ISMA, KU Leuven
3. Rixen DJ (2010) Substructuring using impulse response functions for impact analysis. In: IMAC-XXVIII: international modal analysis conference, Jacksonville, Society for experimental mechanics, Bethel